Sediment and nutrient dynamics during storm events in the Enxoé temporary river, southern Portugal

Tiago B. Ramos[1] Maria C. Gonçalves[2,*], Maria A. Branco[2], David Brito[3], Sara Rodrigues[2], José-Miguel Sánchez-Pérez[4,5], Sabine Sauvage[4,5], Ângela Prazeres[2], José C. Martins[2], Manuel L. Fernandes[2], Fernando P. Pires[2]

[1] CEER, Institute of Agronomy, Technical University of Lisbon, Lisbon, Portugal.

[2] INIAV, Instituto Nacional de Investigação Agrária e Veterinária, Oeiras, Portugal.

[3] IST, Instituto Superior Técnico, Technical University of Lisbon, Lisbon, Portugal.

[4] Université de Toulouse, INPT, UPS, Laboratoire Ecologie Fonctionelle et Environnement (ECOLAB), Ecole Nationale Supérieure Agronomique de Toulouse (ENSAT), Castanet Tolosan, France.

[5] CNRS, Laboratoire Ecologie Fonctionnelle (ECOLAB), Castanet Tolosan, France.

[*] Correspondence to: Maria da Conceição Gonçalves, Instituto Nacional de Investigação Agrária e Veterinária, Quinta do Marquês, Av. República, 2784-505, Oeiras, Portugal. E-mail: maria.goncalves@iniav.pt

ABSTRACT

In temporary rivers the first flood event after a dry period are responsible for transferring significant amounts of sediments and nutrients into water reservoirs, thereby justifying close monitoring. The Enxoé river (southern Portugal) was monitored for suspended sediment concentration (SSC), total phosphorous (TP), particulate phosphorous (PP), soluble reactive phosphorous (SRP), and nitrate (NO_3^-) between September, 2010 and August, 2013. Twenty-one flood events were observed. An empirical model was used to describe changes in solute concentrations, and the magnitude and rotational patterns of the hysteretic loops during flood events. SSC, TP, PP, SRP, and NO_3^- varied between 1.6–1447.9, 0.05–5.15, 0–4.77, 0–0.67, and 0–27.84 mg L^{-1}, respectively. Sediment and phosphorous transport was influenced by the stream transport capacity and particle availability, whereas nitrate loads were influenced by soil hydraulic characteristics and land management. Annual sediment (9.3–338.2 kg ha^{-1} y^{-1}) and nitrate (3.24–33.70 kg ha^{-1} y^{-1}) yields were low, while phosphorous losses (0.03-0.65 kg ha^{-1} y^{-1}) were medium average. Flood events were responsible for the majority of sediment and phosphorus transport (>55.8%), while NO_3^- reached the river mostly through subsurface flow (>84.8%). The implementation of conservation practices, such as no-tillage techniques and the preservation of the riparian vegetation should reduce sediment and nutrient loads to the reservoir. This work highlights the main processes involved in sediments and nutrients loads in a temporary river during flood events, with a precise quantification of those elements.

Keywords: Flood events; Hysteresis; Nitrate; Phosphorous; Suspended sediments.

1. INTRODUCTION

Suspended sediment transport from agricultural catchments to stream networks is responsible for aquatic habitat degradation, reservoir sedimentation and the transport of sediment-bound pollutants (pesticides, particulate, nutrients, heavy metals and other toxic substances). Flood events are a natural phenomenon responsible for driving those sediments and nutrients into streams and lakes. Such events result in pollution peaks that can last from a few minutes to a few days, leading to the eutrophication of water bodies, and to the contamination of drinking water and ecosystems (Langlois *et al*., 2005; Yevenes and Mannaerts, 2011). In the particular case of southern European regions, flood events appear to contribute substantially to phosphorous and nitrogen removal due to the characteristics of the Mediterranean climate and soils, as well as land use (Torrent *et al*., 2007). Phosphorous, which is usually considered the limiting nutrient to primary production, is normally transferred from agricultural soils through runoff and soil erosion, as inorganic P forms bind preferentially to soil sediments through interactions with iron or aluminium (Skoulikidis and Amaxidis, 2009; Oeurng *et al*., 2010a; Zhu *et al*., 2012). Nitrogen, which may also play an important role in autotrophic production, namely in the nitrate form, is more often transported in drainage water (Sánchez-Pérez *et al*., 2003; Buda and DeWalle, 2009; Oeurng *et al*., 2010b; Cerro, 2013).

However, finding a direct relationship between flood events and water quality deterioration is not straightforward as it depends on the catchment topography, hydro-morphology, land use and management, and the remobilisation of sediments and pollutants (Klein and Koelmans, 2011; Zhu *et al*., 2012). These complex relationships are even more undetermined in catchments with temporary rivers located in semi-arid regions where those phenomena remain largely unassessed (Alexandrov *et al*., 2003;

Rovira and Batalla, 2006; Torrent *et al*., 2007; Butturini *et al*., 2008). In these water scarce regions studies with a high sampling density focusing on the hydrological and biogeochemical regimes of temporary rivers are very rare, but are crucial for implementing effective conservation measures and other good agricultural practices.

Over an annual cycle, temporary streams form small lentic shallow systems where sediments and nutrients accumulate, and lotic systems where high flushing rates are often registered (Lillebø *et al*., 2007). During dry periods with flow cessation followed by pool formation, the shallowness of the water column associated with the low discharge and high temperatures may enhance important biochemical processes at the sediment/water column interface leading to the accumulation of nutrients. During flood events, surface or subsurface flow becomes more enriched with sediments and dissolved nutrients accumulated in those pools with severe implications to the physical and chemical environment of the water bodies. Hence, nutrient dynamics in these temporary streams is mainly determined by sequences of dry periods and the following flood events (Lillebø *et al*., 2007), providing a significant challenge in developing sustainable water management plans (Tzoraki and Nikolaidis, 2007).

Monitoring programs are thus essential for understanding the hydrological regime of a temporary river, and the sediment and nutrient dynamics across the catchment. Long-term nutrient concentrations datasets are important to understand nutrient trends, loads, nutrient behaviour, the effectiveness of past nutrient migration and supporting data for future management decisions regarding issues of eutrophication and nutrient control (Burt, 2003; Oeurng *et al*., 2010b). Nevertheless, while monitoring of nutrient concentration is important in determining the nutrient status of a water body, it does not necessarily provide information on the source of those sediments and nutrients. That information is often obtained by analyzing the hysteresis in the concentration-discharge relationship (House and Warwick, 1998; Bowes *et al*., 2005; Eder *et al*., 2010; Oeurng *et al*., 2010a).

This study analyses the temporal variability of suspended sediments concentration (SSC), phosphorous (in both soluble and particulate forms), and nitrate (NO_3^-) in the Enxoé river, southern Portugal. The Enxoé reservoir exibits the highest eutrophic state in Portugal, where many others are also classified as eutrophic (CCDR Alentejo, 2005; Instituto da Água, 2008).

The objectives of this paper are: (i) to present the temporal variability in suspended sediments, soluble and particulate phosphorous forms, and nitrate transport in the Enxoé river (Alentejo region, southern Portugal) during three hydrological year (September, 2010 to August, 2013); (ii) to determine sediment and nutrient loads to the Enxoé reservoir at the outlet of the watershed during the monitored period; and (iii) to identify sediment and nutrient source areas and processes associated based on the interpretation of hysteresis in the concentration-discharge relationship. The results permit to have data on sediment and nutrients loads during storm events in the case of temporary rivers and pretend to help decision-makers to improve the management of drinking water catchments areas by minimizing pollution risks during flood events and reducing the trophic state of freshwater reservoirs.

2. MATERIAL AND METHODS

2.1. Catchment description

The Enxoé catchment is located in the Alentejo region, southern Portugal (Figure 1). The river is a tributary of the Guadiana river, and has a bed length of 9 km, a catchment area of 6080 ha, and an average altitude of 200 m.

The dominant soils are Luvisols (covering 47% of the area), Cambisols (31%), and Calcisols (14%). The main land uses are olive groves (1830 ha), agro-forestry of holm-oaks “Montado” (1760 ha), and annual winter crops (1700 ha). The main agricultural practices are summarized in Table I. The main pressures are essentially originated from non-point sources with loads arriving along the margins of the river (associated to surface or subsurface flow). Average fertilization inputs are estimated to amount 25.40 kg N ha^{-1} and 11.68 kg P ha^{-1} (Table I). Additionally, based on Livestock Units (LSU) presented in Table I, animal excretions are estimated to reach 25.69 kg N ha^{-1} and 3.04 kg P ha^{-1} (Portaria 259/2012). Therefore, nutrient inputs in Enxoé catchment can be considered low since more intensive agricultural catchments are normally characterized by much higher N and P inputs (e.g., Yevenes and Mannaerts, 2011).

The climate is dry sub-humid to semi-arid. The precipitation regime is characterized by a highly irregular behaviour, varying between relatively abundant rainfall episodes, concentrated in only a few minutes or hours, and frequent drought episodes that can last from a few months to a couple of years. The annual average precipitation is 500 mm, irregularly distributed along the year (80% of the annual precipitation is concentrated between October and April). Thus, the hydrological regime presents a strong inter and intra-annual variation of the discharges. From fall to spring, the river frequently presents high flow discharges after storm events. During summer, the river normally exhibits no flow. The annual average temperature is 16 °C, and the annual reference evapotranspiration varies between 1200 and 1300 mm. Weather data used in this study was collected from a weather station located in Serpa (37º 58' 06" N and 07º 33' 03" W).

The catchment has a population of 1000 inhabitants, mainly concentrated in Vale de Vargo (Figure 1), and is limited downstream by a dam (10.4 million m^3) built in 2000, which supplies the villages of Mértola and Serpa (25000 inhabitants) located outside the catchment area. Immediately after the reservoir was built cyanobacteria blooms (up to 300 μg L^{-1}) occurred due to phosphorous overloads and the eutrophication of the reservoir waters. Since then, management actions were implemented in the area, namely, the building of small ditches to control flood events and prevent materials to be carried out from upland to the water reservoir, and the pumping of the waste waters of the treatment plant of Vale de Vargo to a water stream located outside the Enxoé catchment area. Nonetheless, the reservoir continues to be classified as eutrophic.

2.2. River Enxoé water quality monitoring

The river Enxoé water was monitored at the sampling station located at the outlet of the watershed before the reservoir (Figure 1). Sampling waters was for suspended sediment concentration (SSC), total phosphorous (TP), particulate phosphorous (PP) consisting of phosphorous adsorbed to particulate (>0.45 µm) suspended material, soluble reactive phosphorous (SRP), and nitrate (NO_3^-). An YSI 6920 measuring probe (YSI Incorporated, Ohio, USA) was used to monitor the water stream level and turbidity (nephelometry). An automatic water sampler (EcoTech Umwelt-Meßsysteme GmbH. Bonn, Germany) with 8 bottles, 2 L each, was used for monitoring water quality during floods. The monitoring station was positioned near the bank of the river, where the homogeneity of water movement was considered representative of all hydrological conditions. The pump inlet of the automatic water sampler was placed next the measuring probe pipe. The probe was programmed to activate the automatic water sampler when the water level varied more than 10 cm on both rising and falling stages of flood events. Manual sampling was also carried out at weekly intervals using 2 L bottles collected near the probe location. The total number of water samples taken from both automatic and manual sampling was 191. Flow was obtained from the measured water level with the well established Gauckler-Manning formula.

Water samples (250–1000 ml) were filtered in the laboratory to determine SSC using pre-weighted glass microfiber paper (GFF 0.75 µm). The sediments retained on the filter paper were oven dried at 50º C during 24 h. The filters were again weighted and SSC was calculated.

Aliquots of each sample were filtered using a cellulose acetate membrane (0.45 µm), and analyzed for total dissolved phosphorous (TDP), SRP, and NO_3^-. TP was determined in the unfiltered samples. TP and TDP were quantified, after sulfuric acid and nitric acid digestion, colorimetrically by reacting with ammonium molybdate. SRP was also quantified colorimetrically, using the same reaction (APHA, 1995). PP was determined from the difference between TP and TDP concentrations. NO_3^- concentration was measured directly in the filtered solution with an automated segmented flow analyser, using the cadmium reduction method (Hendrilsen and Selmer-Olsen, 1970).

2.3. Water, sediment, and nutrient loads

Water yield was determined by integrating river discharge over a time period, as follows:

$$W = \sum_i \frac{\left(Q_{(i)} + Q_{(i-1)}\right)}{2} \times \left(t_{(i)} - t_{(i-1)}\right) \tag{1}$$

where W is the accumulated water yield (L^3), and Q_j is the instantaneous river discharge (L^3 T^{-1}) at time i (T). Sediments and nutrient loads were obtained by integrating sediment and solute concentrations over water yield, as follows:

$$M_d = \sum_i \frac{\left(C_{d\,(i)} + C_{d\,(i-1)}\right)}{2} \times W_i \qquad (2)$$

where M_d is the solute mass lost in the catchment from diffuse (d) sources (M), and C_j is the instantaneous solute concentration (M L^{-3}) at time i (T). As referred above there are no point source emissions in Enxoé.

A linear interpolation procedure was applied between two neighboring instantaneous sampling points to develop continuous sediments and nutrient series. This was only possible due to the high frequency of data collection provided by the automatic sampler. Turbidity measurements were taken every 3 min to 1 hour during flood events and daily during non-flood events. This quasi-continuous turbidity recording has been shown to reduce significantly uncertainty due to interpolation and extrapolation of low-frequency measurements (Langlois *et al.*, 2005; Lefrançois *et al.*, 2007; López-Tarazón *et al.*, 2009; Eder *et al.*, 2010; Oeurng *et al.*, 2010a). This data was used to determine suspended sediment (SSL) and phosphorous loads based on SSC-turbidity and TP-turbidity relations found in Enxoé. Nitrate was measured directly in the water samplers taken every 3 min to 15 hours during flood events and weakly during non-flood events.

2.4. Solute-discharge hysteresis analysis

For each flood event, the analysis of the concentrations (C) of SSC, TP, PP, SRP, and NO_3^- versus discharge (Q), was performed with the approach proposed by Butturini *et al*. (2006). The shape, rotational patterns and trends of hysteretic loops of each determinand are here described with two parameters: the changes in solute concentrations (ΔC), and the overall dynamics of each hysteretic loop (ΔR).

ΔC (%) describes the relative changes in solute concentration and hysteresis trend, as follows:

$$\Delta C = \left(C_s - C_b\right)/C_{\max} * 100 \qquad (3)$$

where C_b and C_s are the solute concentrations at base flow and during peak storm flow, respectively, and C_{max} is the highest concentration observed in the stream during a storm. ΔC ranges from -100 to 100%, where positive values indicate solute flushing, and negative values solute dilution. The ΔR (%) descriptor integrates information about the magnitude (area) and direction (rotational pattern) of the *C*-*Q* hysteresis, as follows:

$$\Delta R = R\ A_h\ 100 \qquad (4)$$

where A_h is the area of the *C*-*Q* hysteresis, estimated after standardizing discharges and concentrations to a unity scale, which means that A_h will be lower than the unity. If A_h is closer to zero, the area of the hysteresis loop is smaller, more linear, and the concentration in the rising limb is similar to the concentration in the recession limb. If A_h is closer to the unit, the area of the hysteresis loop is larger, with more magnitude, and the concentration of the rising limb is different from the concentration in the recession limb. *R* summarizes the rotational pattern of the *C*-*Q* hysteresis. If the *C*-*Q* hysteresis is clockwise, then R=1; if anticlockwise, then R=-1; for unclear (for example, eight-shaped hysteresis loops) or non-existent hysteresis, R=0. ΔR thus ranges also from -100 to 100%.

The variability of the *C*-*Q* hysteresis descriptors for the different determinands is described in the unity plane ΔC vs. ΔR, where four regions can be identified, according to flushing/dilution of the constituent and the hysteresis loop sense (clockwise or anticlockwise). All this information allows clarifying the source of solutes and particulate matter, and separating different kind of floods. Further details can be found in Butturini *et al*. (2006, 2008).

3. RESULTS

3.1. General description of monitored flood events

Twenty-one flood events were registered between September, 2010 and August, 2013 (Figure 2). These events took place during autumn (10), winter (8), and spring (3), and were defined as complete hydrological events with rising and recession limbs. During summer there was no flow in the river.

Table II summarizes the main characteristics of all flood events monitored. Major rainfall events generally occurred in autumn (October/December) and spring (March/April). Flood events lasted between 1.8 and 210.5 h (mean=67.1 h; standard deviation, σ=45.1 h). Eight events lasted longer than the average duration. Maximum hourly discharge varied between 2.4 and 28.0 $m^3\ s^{-1}$ (mean=7.7 $m^3\ s^{-1}$; σ=5.8 $m^3\ s^{-1}$). Several events produced multiple discharge peaks. The mean rising time to reach the first discharge peak was 8.5 h (σ=6.9 h). The shortest time was only 1 h. Water yield ranged from 10.0 to 2823.7 dam^3 (mean=560.2 dam^3; σ=662.6 dam^3). Six events produced higher water yields than average.

Precipitation amounted 695, 270, and 570 mm in 2010/2011, 2011/2012, and 2012/2013, respectively, thus classifying the corresponding monitored years as humid, dry, and average. Annual water yield was 28737.9 (2010/2011), 1269.8 (2011/2012), and 10138.8 dam^3 (2012/13) corresponding to 62.6, 6.5, and 26.5% of the water budget outputs, respectively.

3.2. Temporal variation of suspended sediments, phosphorous forms and nitrate concentrations

Figure 3 presents the evolution of SSC and turbidity between September, 2010 and August, 2013. Generally, SSC was at a minimum (2.0–215.0 mg L^{-1}) during non-flood events and at a maximum (1.6–1447.9 mg L^{-1}) during flood events. For all hydrological periods, SSC averaged 187.4 mg L^{-1} (σ=269.6 mg L^{-1}). The maximum value was reached in April, 2011 (event nº 9). Higher suspended sediment concentration generally coincided with higher rainfall intensities as in Nadal-Romero *et al*. (2008). Turbidity values followed the same tendencies observed for SSC. However, the maximum value (1520.3 NTU) was observed in October, 2012 (event nº 13). During the monitored period, turbidity averaged 22.8 NTU (σ=55.0 NTU).

Figure 4 presents TP, SRP, PP, and NO_3^- concentrations monitored during the studied period. P concentrations varied between flood events and seasons, decreasing from autumn to winter and increasing again during spring. Maximum values were again observed during flood events. TP values ranged from 0.05 to 5.15 mg L^{-1} (mean=0.94 mg L^{-1}; σ=0.83 mg L^{-1}). PP varied from 0 to 4.74 mg L^{-1} (mean=0.60 mg L^{-1}; σ=0.74 mg L^{-1}). Both maximums were obtained in October, 2010 (event nº 2), when SSC also reached a high value. SRP ranged from 0 to 0.67 mg L^{-1} (mean=0.22 mg L^{-1}; σ=0.16 mg L^{-1}). The highest values were observed again during flood events. The maximum value was reached again in October, 2010 (event nº 2). TDP varied between 0.01 and 1.34 mg L^{-1} (mean=0.34 mg L^{-1}; σ=0.26 mg L^{-1}). SRP contribution to TDP varied between 49% and 97%, while PP fraction constituted the major proportion of TP during most events, averaging 56.3%. SRP constituted only a small fraction of TP, but reached values >35% in 6 events. Since SRP is directly adsorbed by algae, these events may have had a more negative contribution to the eutrophication of the Enxoé reservoir than all the remaining events. Nitrate (NO_3^-) varied between 0 and 27.84 mg L^{-1} (mean=8.02 mg L^{-1}; σ=4.99 mg L^{-1}). The maximum value observed was reached in November, 2010 (also during event nº 2).

Figure 5 presents the relations found for SSC–turbidity (R^2=0.861), for SSC–TP (R^2=0.850), and for SSC–PP (R^2=0.822). These relations suggested that turbidity could also be used to indirectly estimate TP (R^2=0.803). These relations also confirmed that the major portion of P was adsorbed onto suspended solids.

3.3. Suspended sediments, total phosphorous and nitrate loads assessment

Figure 6 presents the cumulative suspended sediment and nutrient loads to the Enxoé reservoir from September, 2010 to August, 2013. Table III shows the same sediment and nutrient yields by flood event. The results demonstrate the strong seasonal and annual variability in suspended sediment, phosphorous, and nitrate transport in the Enxoé catchment. Sediment transport during flood events ranged from 1.4 to 543.4 t (mean=115.6 t; σ=159.0 t), and was higher during autumns and springs. Maximum load was obtained in March, 2013 (event nº 18), which also corresponded to the event with maximum water yield (2823.7 dam^3). Minimum load was observed in October, 2011 (event nº 10) during a drought period. Annual sediment yield accounted for 1146.9, 56.3, and 1277.5 t in 2010/2011, 2011/2012, and 2012/2013, respectively. Flood events were thus responsible for 55.8, 5.7, and 76.8% of the annual sediment transport. On the other hand, water yield during flood events only amounted 18.7, 18.0%, and 60.9% of each year's annual flow.

The temporal dynamics in phosphorous transport was similar to suspended sediment since both particulate elements were taken directly from turbidity measurements. Phosphorous transport during flood events ranged from 4.2 to 1356.3 kg (mean=301.5 kg; σ=382.5 kg). Flood events were responsible for 82.4, 5.24, and 80.4% of the annual phosphorous transport in 2010/2011, 2011/2012, and 2012/2013, respectively. Phosphorous transport also showed to be dependent on the intensity and amplitude of the flood events as higher loads corresponded generically to larger water yields.

Nitrate loads also demonstrated large seasonal and annual variability. Nitrate yield was higher mainly during autumns, but also during springs. The nitrate load transported during observed flood events varied from 0.04 to 10.2 t (mean=2.7 t; σ=3.2 t). The highest nitrate load (10.2 t) was transported in October, 2010 (event nº 2). Nitrate transport during flood events amounted 30.9 (2010/2011), 3.3 (2011/2012), and 12.7 t (2012/2013) while the annual nitrate yield summed 204.8, 19.7, and 67.8 t, respectively. Thus, flood events were directly responsible for only 15.2, 16.9, and 18.1% of each year's annual load, i.e., the most significant loads reached the river during non-flood events (with the exception of summer seasons).

From December 19th, 2010 to January 9th, 2011 it was not possible to measure turbidity directly with the automatic probe due to equipment malfunctioning. Loads were therefore estimated from the statistical relationship between SSL (or total phosphorous) and discharge obtained during the remaining monitored period (Figure 7). The relationship between SSL or phosphorous loads (or concentrations) and discharge is generally represented by a power function (Langlois *et al*., 2005; Lefrançois *et al*., 2007). However, in this case, the SSL-discharge and TP-discharge was polynomial, i.e., only high discharges led to significant sediment and phosphorous transport since they were normally a function of the transport capacity of a river (Asselman, 1999). However, the relationships found do not include high sediment and phosphorous loads measured in low discharges, i.e., it cannot represent hysteresis events. Therefore, the polynomial relations described in Figure 7 can eventually lead to underestimations of sediment and nutrient loads during the time period (22 days) when the equipment malfunctioned.

3.4. Hysteresis patterns

The relationships between discharge and SSC, TP, PP, SRP, and NO_3^- were analyzed for most events observed in the Enxoé catchment. Those that did not produce sufficient detailed information, as a result of equipment malfunctioning or data limitation (soluble elements) were not analyzed for their hysteresis patterns.

Figure 8 shows the unity plane ΔC vs. ΔR of Butturini *et al*. (2006), and summarizes *C*-*Q* hysteresis loop types of the particulate determinands (SSC, TP, and PP) during the monitored flood event. The components of the particulate matter were located in regions A and D, indicating a flushing behavior (positive ΔC). Obviously, SSC, TP, and PP presented similar or equal hysteresis loops during each discharge peak, and were thus located very close to each other in the unity plane ΔC vs. ΔR. Most flood events registered during autumn were located in region A, presenting a clockwise hysteresis loop trajectory (positive ΔR). Events nº 15 and 16 were the exception, registering anticlockwise loop trajectories in all discharge peaks (region D). Winter flood events registered mixed (eight-shaped hysteresis loops; ΔR=0) or anticlockwise loop trajectories (negative ΔR). Spring flood events showed contrasting behaviors with the event observed during the first hydrological year revealing an anticlockwise trajectory and the events observed during the third hydrological year presenting anticlockwise trajectories.

Generally, the first peaks of autumn flood events showed larger dispersion of the *C*-*Q* hysteresis loops when compared with the remaining events. Those peaks presented a large area (Δ*R*>20%) while all other events had a smaller magnitude (-20%<Δ*R*<20%). Thus, autumn floods were responsible for transferring more particulate elements from the soil to the reservoir than the remaining events. Also, many events (especially those that occurred during winter) presented a Δ*C* near 100% indicating that the hysteresis patterns presented a coincidence between the maximum concentration values and maximum discharge, i.e., the delay between concentration and discharge peaks was small.

Figure 9 shows the unity plane Δ*C* vs. Δ*R* for the soluble elements (SRP, and NO_3^-) monitored. SRP was located in all regions of the unity plane leading to some uncertainty when analyzing its hysteresis patterns. Nevertheless, SRP seems to generically have registered a dilution behavior (negative Δ*C*) during autumn and a flushing behavior (positive Δ*C*) during winter and spring. Most autumn flood events also showed contrasting hysteresis patterns, but during winter and spring most hysteresis loops were clockwised (Δ*R*>0).

NO_3^- were located in regions B, C, and D in the unity plane Δ*C* vs. Δ*R*. Autumn flood events autumn presented, in general, a flushing behavior (positive Δ*C*) and an anticlockwise trajectory (negative Δ*R*). Those *C*-*Q* hysteresis loops revealed a large magnitude (Δ*R*<-20%) indicating large transfer of nitrate in the catchment area during autumn which is in agreement with load estimates presented above. The remaining flood events showed a dilution behavior (negative Δ*C*) and anticlockwise trajectories.

4. DISCUSSION

4.1. Hydrological behavior

The Enxoé river is a temporary river that normally exhibits no flow or ephemeral conditions from June to October. In each monitored hydrological year, the first rain events generated flow peaks that were quickly reduced as the soil was not saturated and groundwater flow was greatly diminished. From October to December, with successive heavy rains the soil became increasingly saturated and subsurface flow was enhanced, resulting most times in flood events with multiple discharge peaks. From December/January to April, the response to rain events still existed as the soil continued to be saturated and groundwater flows were maintained for longer periods. However, these subsurface flows still tended to fall quickly, especially during months in which rain was less intense (January/February). Hence, flow in the river Enxoé was mostly influenced by rainfall events, whereas the effect of groundwater table was not significant.

Table IV presents the relationships between floods and rainfall events. Floods duration (*FD*) were mainly correlated with water yield (*W*), the rainfall amount registered between the rising and recession limbs of a flood event (*TR*), the size of the first discharge peak (P_{max}), and the time to reach it after the start of the rainfall event (T_{peak}). *TR* was further related to the amount of precipitation registered in the 24 h prior to an event (*R1*). Thus, the stream transport capacity of the Enxoé river was indirectly influenced by *R1*. Finally, *W* and the average discharge of a flood event (P_{aver}) were also strongly related.

4.2. Sediment and nutrient dynamics

4.2.1. Suspended sediments

The strong seasonal and annual variability observed in SSC was mostly explained by variations in stream transport capacity and particle availability. Sediment was stored at low flow and transported under high discharge conditions. Heavy rains registered during autumn and tillage operations carried out simultaneously in agricultural area

(Table I) enhanced soil erosion. Tillage operations were thus an important mechanism associated to sediment transport. They ended up promoting the removal of the soil cover surface provided by crop residues or growing plants which absorb the energy of raindrops and reduce the cutting energy of runoff during rain events.

Another important mechanism associated to sediment transport during autumn was related to bank destruction or trampling caused by cattle pasturing near the river during drier seasons. Bull (1997) estimated that the contribution of bank eroded materials to river sediment systems may vary between less than 5 to over 80%. Pasturing near streams, or even in the river bed, leads to vegetation reductions, affecting flow erosion, bank stability, bank accretion, and bank stabilization. Bull (1997) also refers the mechanisms on how vegetation contributes to prevent bank erosion, namely, by retarding the near-bank flow and damping turbulence, by resisting tension and increasing cohesion, and by reducing the impact of moisture and loosening processes, which are a precursor to removal of materials. Therefore, pasturing the river bed promotes bank erosion, with the ruined bank materials adding to the deposited sediment stock to increase the quantity of available particles that can be easily transported (Lefrançois *et al*., 2007). Thus, at the beginning of autumn, particle availability is at maximum. The first flood events are then responsible for significant loads to the reservoir. These conditions explain the dominant clockwise loop trajectories and the flushing effect registered during the first peak discharge of autumn floods (Table V). Multiple discharge peaks can then be responsible for carrying sediment from multiple locations (arable lands located upstream) or from new deposited originated from a high rate of bank collapse just after the passage of the first flood peaks (Asselman, 1999).

During winter, sediment loads remained generally low. Asselman (1999) observed that in a situation where storm events occur in rapid succession (e,g., October/November, 2012), SSC loads become progressively reduced because of insufficient time for exhausted sediments to accumulate between events. Sediment transport is originated from more distant locations, namely soil erosion in agricultural fields, as confirmed by the anticlockwise or mixed patterns registered in the *C*-*Q* relation.

During March and April, sediment loads increased again, as a result of high precipitation values and consequent soil erosion. During these periods, tillage operations are again carried for sowing spring crops like sunflower, weed control, and fire prevention in the agro-forestry of holm-oaks “Montado” system. These practices again promoted particle availability to runoff (flushing). There was also a return of the cattle to pasturing near the stream with consequent bank erosion. Clockwise and anticlockwise trajectory loops were observed whenever sediments were transported from the river deposits or from more distance locations upstream, respectively.

Similar patterns to those observed for SSC in Enxoé have been observed in different regions of the Mediterranean (Rovira and Batalla, 2006; Lefrançois *et al.*, 2007; López-Tarazón *et al.*, 2009; Oeurng *et al.*, 2010a). Based on the hysteretic patterns analyzed in Enxoé, clockwise hysteretic loops represented 46.2% of sediment transport from river deposited sediments and nearby source areas, while anticlockwise loops represented 42.9% of sediment transport from distant source areas. The remaining materials arrived at the outlet in a mixed trajectory, thus the source of these sediments was unclear.

Annual sediment yield varied between 9.3 and 338.2 kg ha^{-1} (Table VI). The lower value was determined during a dry year. Since no major flood events were registered soil erosion was minimal. The value determined in 2010/2011 (338.2 kg ha^{-1}) may be viewed as notably low considering that was obtained in a humid year, but is within the same order of magnitude of the values registered for other catchments in the Iberian Peninsula. Rovira and Batalla (2006) estimated a sediment loss of 500 kg ha^{-1} in a catchment located in Cataluña, Spain. In this catchment, more than 90% of the annual sediment load was transported during flood events. Casalí *et al*. (2010) also reported sediment losses of 550-700 kg ha^{-1} yr^{-1} in two catchments located in Navarre, Spain. Nonetheless, Walling and Webb (1996) described sediment losses between 1000-2000 kg ha^{-1} yr^{-1} for other Mediterranean basins of the Iberian Peninsula. The values determined in Enxoé also fall within the lower values obtained by de Vente *et al*. (2006) for 44 Mediterranean basins in Italy. Oeurng *et al*. (2010a) also reported sediment losses of 150-700 kg ha^{-1} for a catchment located in the south of France, in which 85-95% of the annual sediment load was transported during flood events.

The Enxoé catchment presents a significant area with agro-forestry of holm-oaks "Montado" (1760 ha) that plays an important role in protecting soil surface from soil erosion due to the reduced number of tillage operations carried out there. It explains mostly the low sediment yield losses registered in Enxoé. Rovira and Batalla (2006), Casalí *et al*. (2010), and Oeurng *et al*. (2010a) also reported significant areas with forests or pastures that contributed similarly to soil protection. While sediment losses in Enxoé were within the threshold limits (1000-2000 kg ha^{-1} yr^{-1}) suggested by Huber *et al*. (2007) to be considered as tolerable for the south of Europe, results represent an average value for the entire catchment. Naturally, sediment yield was higher in areas with arable land than in areas with agro-forestry systems or even olive groves. It is therefore important to adopt preventing measures for reducing soil erosion in those arable areas. Reduced tillage (or no-till) can be effective in reducing sediment losses by maintaining crop residue on the soil surface and minimizing soil particle movement during storms. These techniques are also known to improve water infiltration by promoting soil aggregation which would obviously contribute to reducing runoff. On the other hand, hysteresis patterns showed that there is a significant contribution (46.2%) from nearby sources to sediment loads during storm events. Therefore, river banks need simply to be protected from pasturing with consequent improvement of bank stability and cohesion.

4.2.2. Phosphorous forms

Total and particulate phosphorous dynamics revealed the same patterns as observed for SSC since both were obtained from turbidity measurements. The same clockwise and anticlockwise flushing effects referred earlier for SSC were also observed here (Table V). SRP increase during autumn was mostly related to the application of P to crops. During spring, P may also be supplied (Table I). Nonetheless, the clockwise trajectory observed during winter and spring floods seems to be mostly justified by the return of the cattle pasturing near the stream and eventual increase of SRP concentration in the river (Table VI).

Annual phosphorous losses varied between 0.03 and 0.65 kg ha^{-1} during the monitored period (0.2-4.4% of P inputs; Table VI). The lower value was again determined when no major flood events were registered (2011/2012). P loads observed in 2010/2011 and 2012/2013 can be considered within the average of reported P losses. Casalí *et al*. (2010) presented slightly higher values (0.76 kg P ha^{-1} yr^{-1}) in one of the catchments studied in Navarra (Spain), but found lower P exports (0.35 kg P ha^{-1} yr^{-1}) in the other catchment studied in the same region. Tzoraki and Nikolaidis (2007) only found loads of 0.10 kg P ha^{-1} (1.2% of input) in a mountain forested catchment in Greece. Probst (1985) reported equally low exportation rates (1%) for his case study. Klein and Koelmans (2011) reported data on P exports (0.08-0.88 kg P ha^{-1} yr^{-1}) for 13 central European basins, in which the Enxoé values would fall within the mean. Nonetheless, all these values are much lower than the 1.2-1.7 kg P ha^{-1} yr^{-1} loads reported in the UK by Brazier *et al*. (2005).

Although phosphorous loads to the Enxoé reservoir were within the average of reported values, they may help explaining the frequent toxic algae bloom observed in the reservoir since its construction. However, the most significant part arrived at the reservoir in the particulate form and was therefore deposited at the bottom being only available to algae after mineralization. The same practices (reduced tillage and river bank protection) recommended earlier for controlling soil erosion can also be adopted for reducing P loads to the reservoir. Specifically, preserving the riparian vegetation will play here a fundamental role in retaining part of the phosphorous particles deposited in the river.

4.2.3. Nitrate

Hydrology was the most important factor influencing the processes responsible for the removal of the nitrate resulting from agricultural practices (Sánchez-Pérez *et al*., 2003; Ocampo *et al*., 2006). Rainfall and soil hydraulic characteristics were here the main characteristics influencing nitrate transport. On the other hand, land management, namely crop fertilization periods, influenced nitrate availability.

Nitrate losses were mostly monitored during autumn and spring. These two seasons registered the most important rainfall events and corresponded to crop fertilization periods. During autumn, fertilization was applied to annual winter crops during sowing, which normally involved burying fertilizers, thus preventing N losses by runoff. During late-winter/spring, fertilization was applied to summer crops also during sowing. Additionally, annual winter crops were fertilized to promote tillering

(February/March) and increase crop yield. However, fertilizers were here usually applied to the soil surface, increasing the odds of N losses by runoff (e.g., event nº 7) as well as leaching with rainfall.

Hysteresis patterns observed during the monitored events showed predominantly anticlockwise trajectories. NO_3^- infiltrated first in the soil only reaching later the water stream through subsurface flow. Nitrate transport was thus dependent of the soil physical and hydraulic characteristics, i.e., soil texture, soil porosity, soil water retention, and soil hydraulic conductivity, which influenced water flow and mass transport and produced a delay in the concentration-discharge peak. Buda and DeWalle (2009), Oeurng *et al*. (2010b), Zhu *et al*. (2012) registered similar preferential flowpaths with nitrate losses being associated to either subsurface flow or baseflow.

Hence, peak discharges were not directly associated to nitrate transport with only 15.2-18.7% of the annual yield being monitored during flood events (Table III). The flushing effect and the anticlockwise loops observed during autumn (Figure 9) showed that significant amounts of nitrate were transported from distant areas of the catchment in the days after those flood events, namely from the agricultural fields where fertilization occurred. This flushing mechanism was explained by the successive rainfall events registered during that period, soil moisture close to saturation, and the medium to coarse textures of the relatively shallow soils in the catchment, namely Luvisols and Cambisols which totalize 78% of the area. This characteristics favored subsurface water flow from a significant part of the area, removing significant amounts of nitrate applied to annual winter crops during sowing.

During winter and spring the flushing mechanism switched to a dilution behavior (Table V). Nitrate concentrations in the river always decreased with the arrival of the discharge peak, that is, nitrate concentration in surface runoff was lower than in subsurface flow. Hence, there was no nitrate being transported across the catchment with the exception of that due to the soil leaching had origin in the annual winter crop areas. The arrival of “clean” water from non-fertilized areas, such as agro-forestry of holm-oaks “Montado” and permanent pastures partially diluted river flow.

Nitrogen inputs to the catchment amounted 51.10 kg N ha^{-1}, applied under different N forms either from fertilization or livestock (Table I). Besides nutrient uptake, various N transformation processes then occurred in soils mostly due to microbial activity which was controlled by soil environmental conditions such as soil water and temperature (Lillebø *et al*., 2007). From the initial inputs, between 0.73 and 7.61 kg N ha^{-1} arrived at the reservoir in the nitrate form, i.e., between 3.24 and 33.70 kg NO_3^- ha^{-1}. Nitrate exports in Enxoé can thus be considered low since agriculture and pasturing are not very intensive. Nitrate loads fall within the same order of magnitude as those found by Oeurng *et al*. (2010b) and Probst (1985) for catchments in the south of France. There, nitrate loads varied from 10-50 kg NO_3^- ha^{-1}. Casalí *et al*. (2010) also reported values ranging from 22-54 kg NO_3^- ha^{-1} in the two catchments studied in Navarre (Spain). In tems of N units, Tzoraki and Niolaidis (2007) reported losses of 2.73 kg N ha^{-1} (11% of input) in their case study (forested areas were here the dominant land use with 75.4% of the area). But, compared with the values Klein and Koelmans (2011) for catchments in Central Europe (0.8-42.6 kg N ha^{-1} yr^{-1}), N exports in the Enxoé catchment are within the lowest values.

The identification of nitrate sources in the Enxoé catchment using hysteresis patterns was relatively clear due to the small size of the catchment and predominant land uses and land management. Nitrate losses were associated to non-point sources but the periods where higher exports were observed always corresponded to fertilization periods of annual winter and summer crops. Nitrate losses were low though but could be further minimized by increasing fertilization efficiency (by reducing applications during rainy years) or by preserving riparian vegetation which would use most of the nitrate exported to the river before it reached the reservoir.

5. CONCLUSIONS

Sediment and nutrient dynamics in the Enxoé catchment showed a strong seasonal and annual variability during the monitored period. Annual discharge varied between 1.2 and 28.7 hm^3 depending on the amount of rainfall registered in each hydrological year.

Annual sediment losses were relatively low (9.3–338.2 kg ha^{-1} y^{-1}) and were related with the amount of rainfall registered each year. Flood events were responsible for 55.8-76.8% of the annual loads to the reservoir. Likewise, annual phosphorous transport was considered to be within the average of reported values (0.03-0.65 kg ha^{-1} y^{-1}), with flood events being responsible for most of P transport (80.2-82.4%). During the monitored period, 46.2% of the sediment and P losses had origin in river bed deposits that had resulted from pasturing the river bed and river banks, while 42.9% were originated from the enhancement of soil erosion due to tillage operations carried out in agricultural fields. Sediment and phosphorous dynamics in the catchment were thus associated to the stream transport capacity and particle availability throughout the seasons.

The behavior of the soluble elements was in general different from the particulate ones. SRP was mostly originated near the river banks. However, a larger number of SRP-*Q* response for Enxoé river is still necessary in order to better identify a "most probable SRP response. Annual nitrate loads were also low (3.24–33.70 kg ha^{-1} y^{-1}), with the highest exports being observed in autumn and spring. However, the contribution of flood events to NO_3^- loads reached only 15.2–18.7% of the annual losses. The most significant part was transported from agricultural fields during non-flood events, through subsurface flow depending on the soil hydraulic characteristics.

Based on the conceptual model developed for Enxoé, the most feasible measure towards reducing eutrophication in the Enxoé reservoir would be the adoption of non-tillage practices which would improve soil stability and increase water infiltration, thus reducing runoff. Also, the protection of the river banks from pasturing, with the consequence preservation of the riparian vegetation, would retain a significant part of the nutrients in the river, improve banks aggregation and stability, and reduce sediment deposits in the river bed.

ACKNOWLEGEMENTS

This research was performed within the framework of the EU Interreg SUDOE IVB program (SOE1/P2/F146 AguaFlash project, http://www.aguaflash-sudoe.eu), and the Project EUTROPHOS (PTDC/AGR-AAM/098100/2008) of the Fundação para a Ciência e a Tecnologia (FCT).

REFERENCES

Alexandrov Y, Laronne JB, Reid I. 2003. Suspended sediment concentration and its variation with water discharge in a dryland ephemeral channel, northern Negev, Israel. *Journal of Arid Environments* **53**: 73-84.

Asselman NEM. 1999. Suspended sediment dynamics in a large drainage basin: the River Rhine. *Hydrological Processes* **13**: 1437-1450.

APHA. 1995. Standard methods. 19th Edition. American Public Health Association, Washington, DC.

Bowes MJ, House WA, Hodgkinson RA, Leach DV. 2005. Phosphorus-discharge hysteresis during storm events along a river catchment: the River Swale, U.K. *Water Research* **39**: 751-762.

Brazier RE, Heathwaite AL, Liu S. 2005. Scaling issues relating to phosphorous transfer from land to water in agricultural catchments. *Journal of Hydrology* **304**: 330-342.

Buda AR, DeWalle DR. 2009. Dynamics of stream nitrate sources and flow pathways during stormflows on urban, forest and agricultural watersheds in central Pennsylvania, USA. *Hydrological Processes* **23**: 3292-3305.

Bull LJ.1997. Magnitude and variation in the contribution of bank erosion to the suspended sediment load of the river Severn, UK. *Earth Surface Processes and Landforms* **22**: 1109-1123.

Burt TP. 2003. Monitoring change in hydrological systems. *The Science of the Total Environment* **310**: 9-16.

Butturini A, Gallart F, Latron J, Vazquez E, Sabater F. 2006. Cross-site comparison of variability of DOC and nitrate C-Q hysteresis during the autumn-winter period in three Mediterranean headwater streams: a synthetic approach. *Biogeochemistry* **77**: 327-349.

Butturini A, Alvarez M, Bernal S, Vazquez E, Sabater F. 2008. Diversity and temporal sequences of forms of DOC and NO3-discharge responses in an intermittent stream: Predictable or random succession? *Journal of Geophysical Research* **113**, G03016. doi:10.1029/2008JG000721.

Casalí J, Giménez R, Díez J, Álvarez-Mozos J, Del Valle de Lersundi J, Goñi M, Campo MA, Chahor Y, Gastesi R, López J. 2010. Sediment production and water quality of watersheds with contrasting land use in Navarre (Spain). *Agricultural Water Management* **97**: 1683-1694.

Cerro I, Sánchez-Pérez JM, Ruiz-Romera E, Antigüedad, I. 2013. Variability of particulate (SS; POC) and dissolved (DOC, NO_3) matter during storm events in the Alegria agricultural watershed. *Hydrological Processes*. doi:10.1002/hyp.9850.

CCDR Alentejo. 2005. Anuário de recursos hídricos do Alentejo. Ano Hidrológico 2003/2004. MAOTDR, Évora, Portugal.

de Vente J, Poesen J, Bazzoffi P, van Rompaey A, Verstraeten G. 2006. Predicting catchment sediment yield in Mediterranean environments: the importance of sediment sources and connectivity in Italian drainage basins. *Earth Surface Processes and Landforms* **31**: 1017-1034.

Eder A, Strauss P, Krueger T, Quinton JN. 2010. Comparative calculation of suspended sediment loads with respect to hysteresis effects (in the Petzenkirchen catchment, Austria). *Journal of Hydrology* **389**: 168-176.

Hendrilsen A, Selmer-Olsen AR. 1970. Automatic methods for determination of nitrate and nitrite in water and soil extracts. *The Analyst* **95**: 514-518.

House WA, Warwick MS. 1998. Hysteresis of the solute concentration/discharge relationship in rivers during storms. *Water Resources* **32**: 2279–2290.

Huber S, Prokop G, Arrouays D, Banko G, Bispo A, Jones RJA, Kibblewhite MG, Lexer W, Möller A, Rickson RJ, Shishkov T, Stephens M, Toth G, Van den Akker JJH, Varallyay G, Verheijen FGA, Jones AR (eds). 2008. Environmental Assessment of Soil for Monitoring: Volume I Indicators & Criteria. EUR 23490 EN/1, Office for the Official Publications of the European Communities, Luxembourg, 339pp.

Instituto da Água. 2008. Poluição provocada por nitratos de origem agrícola. Directiva 91/676/CEE, de 12 de Dezembro de 1991. Relatório (2004-2007). Publicação conjunta do MAOTDR e MADRP, Lisboa, Portugal.

Klein JJM, Koelmans AA. 2011. Quantifying seasonal export and retention of nutrients in West European lowland rivers at catchment scale. *Hydrological Processes* **25**: 2102-2111.

Langlois JL, Johnson DW, Mehuys GR. 2005. Suspended sediment dynamics associated with snowmelt runoff in a small mountain stream of Lake Tahoe (Nevada). *Hydrological Processes* **19**: 3569-3580.

Lefrançois J, Grimaldi C, Gascuel-Odoux C, Gilliet N. 2007. Suspended sediment and discharge relationships to identify bank degradation as a main sediment source on small agricultural catchments. *Hydrological Processes* **21**: 2923-2933.

Lillebø AI, Morais M, Guilherme P, Fonseca R, Serafim A, Neves R. 2007. Nutrient dynamics in Mediterranean temporary streams: A case study in Pardiela catchment (Degebe River, Portugal). *Limnologica* **37**: 337–348.

López-Tarazón JA, Batalla RJ, Vericat D, Francke T. 2009. Suspended sediment transport in a highly erodible catchment: The River Isábena (Southern Pyrenees). *Geomorphology* **109**: 210-221.

MADRP. 2010. Análise dos impactos no solo resultantes da introdução de novos olivais regados no Alentejo. 2º Relatório do Grupo de Trabalho do Olival. INRB, MADRP, Lisboa.

Nadal-Romero E, Regues D, Latron J. 2008. Relationships among rainfall, runoff, and suspended sediment in a small catchment with badlands. *Catena* **74**: 127-136.

Ocampo CJ, Oldham CE, Sivapalan M, Turner JV. 2006. Hydrological versus biogheochemical controls on catchment nitrate export: a test of the flushing mechanism. *Hydrological Processes* **20**: 4269-4286.

Oeurng C, Sauvage S, Sánchez-Pérez JM. 2010a. Dynamics of suspended sediment transport and yield in a large agricultural catchment, southwest France. *Earth Surface Processes and Landforms* **35**: 1289–1301.

Oeurng C, Sauvage S, Sánchez-Pérez JM. 2010b. Temporal variability of nitrate tranport through hydrological response during flood events within a large agricultural cathcment in south-west France. *Science of the Total Environment* **409**: 140-149.

Probst JL. 1985. Nitrogen and phosphorous exportation in the Garonne Basin (France). *Journal of Hydrology* **76**: 281-305.

Rovira A, Batalla RJ. 2006. Temporal distribution of suspended sediment transport in a Mediterranean basin: The Lower Tordera (NE Spain). *Geomorphology* **79**: 58-71.

Sánchez-Pérez JM, Vervier P, Garabétian F, Sauvage S, Loubet M, Rols JL, Bariac T, Weng P. 2003. Nitrogen dynamics in the shallow groundwater of a riparian wetland zone of the Garonne, SW France: nitrate inputs, bacterial densities, organic matter supply and denitrification measurements. *Hydrology and Earth System Sciences* **7**, 97-107.

Skoulikidis N, Amaxidis Y. 2009. Origin and dynamics of dissolved and particulate nutrients in a minimally disturbed Mediterranean river with intermittent flow. *Journal of Hydrology* **373**: 218-229.

Torrent J, Barberis E, Gil-Sotres F. 2007. Agriculture as a source of phosphorus for eutrophication in southern Europe. *Soil Use and Management* **23**: 25-35.

Tzoraki O, Nikolaidis NP. 2007. A generalized framework for modeling the hydrologic and biochemical response of a Mediterranean temporary river basin. *Journal of Hydrology* **346**: 112-121.

Walling DA, Webb BW. 1996. Erosion and sediment yield: A global overview. IAHS Publications 236. IAHS Press: Wallingford, 3-19.

Yevenes MA, Mannaerts CM. 2011. Seasonal and land use impacts on the nitrate budget and export of a mesoscale catchment in Southern Portugal. *Agricultural Water Management* **102**: 54-65.

Zhu Q, Schmidt JP, Bryant RB. 2012. Hot moments and hot spots of nutrient losses from a mixed land use watershed. *Journal of Hydrology* **414-415**: 393-404.

List of Tables

Table I. Summary description of the main agricultural practices carried out in the Enxoé catchment area.

Land use	Tillage operations	Fertilization inputs[a]	Livestock
Olive groves	Traditional olive groves (<100 trees/ha): Harrowing (October) Intensive olive groves (300-500 trees/ha): No tillage; average irrigation depths 200 mm (MADRP, 2010)	Traditional olive groves (<100 trees/ha): 24 units of N (April and May) Intensive olive groves (300-500 trees/ha): 60 units of N (April to July) 15 units of P (April to July) 30 units of K (April to July)	Sheep (0.1 LSU[b])
Agro-forestry of holm-oaks “Montado”	Areas with >30 trees/ha: Harrowing (May) Areas with <30 trees/ha: Include also annual winter crops Harrowing (October)	Annual winter crops: Triticale and Oats 40-80 units of N (October to November) 60 units of P (October to November)	Cows, sheep, goats, and pigs (0.4 LSU, which increase to 0.6 LSU for 3 months during holm-oaks fructification period)
Annual winter crops: Rotation 1 (sunflower + wheat or triticale + barley or oats) Rotation 2 (wheat or triticale + oats + fallow) Rotation 3 (oats + fallow)	Sunflower: Moldboard plowing (April) Harrowing (April) Heavy rolling (April) Sowing (April) Harvest (September) Wheat, Triticale and Barley: Harrowing (November) Sowing (November) Harvest (June) Oats: Harrowing (November) Sowing (October) Harvest (June)	Sunflower: 22 units of P (April) 42 units of K (April) Wheat, Triticale and Barley: 20 units of N (November) 18 units of P (November) 50-90 units of N (January to February) Oats: 40 units of N (March)	Cows and sheep (0.6 LSU)
Permanent Pastures	No tillage operations	18 units of P (October)	Cows and sheep (0.6 LSU)

[a] values obtained by inquiring the farmers in the region.

[b] LSU – Livestock units

Table II. General characteristics of the flood events observed in the Enxoé catchment between September, 2010 and August, 2013[a].

Flood Events		Rainfall								Discharge				
Nº	Date	FD (h)	W (dam^3)	RA (mm)	RD (h)	R1 (mm)	R2 (mm)	R5 (mm)	R10 (mm)	Mean (m^3 s^{-1})	Peak Nº	P_{max} (m^3 s^{-1})	T_{peak} (h)	R_{peak} (mm)
Year: 2010/2011														
1	08/10 - 11/10	51.6	44.7	41.3	3.6	31.4	31.4	31.5	40.6	1.3	1st	3.6	6.0	33.0
2	29/10 - 02/11	81.2	969.2	48.1	2.7	16.6	16.6	16.6	16.7	5.7	1st	5.2	3.0	18.2
											2nd	10.5	15.0	43.4
											3rd	8.2	17.0	46.6
3	18/12 - 23/12	127.1	622.7	84.1	3.7	28.0	28.0	28.3	29	4.7	1st	28.0	24.0	28.0
											2nd	8.3	81.0	51.2
											3rd	8.9	113.0	84.1
4	30/12 - 02/01	92.3	497.3	21.7	3.4	18.8	18.8	18.9	55.9	1.5	1st	4.2	21.0	18.8
5	07/01 - 09/01	70.3	265.1	19.5	2.3	6.4	7.4	13.1	34.8	1.0	1st	3.5	7.0	6.5
6	28/01 - 31/01	90.1	347.4	25.6	3.6	6.4	11.0	13.5	25.5	1.1	1st	5.5	19.0	19.0
7	15/02 - 17/02	71.8	1473.1	28.0	7.2	18.5	19.5	23.5	23.6	5.0	1st	7.2	17.0	10.0
											2nd	9.5	23.0	16.2
											3rd	13.8	45.0	18.7
8	14/03 - 15/03	47.9	975.2	26.0	3.2	27.8	33.0	52.7	93.2	5.7	1st	10.6	7.0	12.6
											2nd	19.7	15.0	24.6
9	19/04 - 21/04	48.0	170.9	75.9	6.6	45.6	45.8	45.8	45.8	0.8	1st	6.2	12.0	38.4
Year: 2011/2012														
10	26/10 - 28/10	29.4	68.6	68.2	4.1	29.3	30.3	30.3	32	0.7	1st	2.4	2.0	65.9
11	09/11 - 10/11	35.5	153.3	40.2	3.5	2.6	2.8	2.9	40.2	0.8	1st	2.4	5.0	40.2
Year: 2012/2013														
12	24/10 - 24/10	1.8	10.0	26.9	1.3	26.9	26.9	27.8	45.9	1.6	1st	3.0	1.0	47.0
13	03/11 - 05/11	59.4	278.1	19.7	5.1	8.4	22.1	33.4	42.8	3.0	1st	4.3	2.0	42.8
14	08/11 - 10/11	45.3	433.2	33.8	2.7	24.2	32.0	43.3	76.7	2.9	1st	12.8	4.5	32.0
											2nd	4.9	37.0	41.5
15	16/11 - 17/11	37.8	145.1	49.4	2.4	40.3	49.2	49.2	90.8	1.1	1st	3.1	2.3	49.2
											2nd	2.7	21.0	58.3
16	15/12 - 17/12	61.0	262.0	18.3	4.7	14.7	17.0	17.4	29.1	1.3	1st	4.2	10.3	17.4
											2nd	2.5	54.8	21.0
17	19/01 - 20-01	20.3	108.9	21.0	1.3	15.7	16.2	17.4	20.5	1.6	1st	3.7	3.0	16.2
18	04/03 - 14/03	210.5	2823.7	85.4	2.1	11.7	12.5	12.7	18.1	2.9	1st	6.4	12.3	12.5
											2nd	5.9	62.7	45.7
											3rd	17.6	91.3	57.6
											4th	5.3	181.0	86.2
19	19/03 - 21/03	51.0	353.8	21.1	2.9	21.1	21.1	23.8	53.5	2.1	1st	8.3	5.8	21.1
20	23/03 - 25/03	51.5	429.4	12.8	2.1	9.8	21.8	42.9	45.6	2.3	1st	4.3	2.5	9.8
21	31/03 - 05/04	124.6	1331.7	45.8	4.7	32.3	32.3	36.7	66.2	3.0	1st	16.4	11.3	32.3

[a] FD, flood duration; W, water yield; RA, rainfall amount between the rising and recession limbs of a flood event; RD, rainfall duration in a flood event; R1, R5, and R10, cumulative precipitation in the 24h, five and ten days before the first discharge peak, respectively; P_{max}, discharge peak; T_{peak} and R_{peak} correspond to the duration and amount of rain accumulated since the beginning of the rain event until the discharge peak of a flood event, respectively.

Table III. Water yield and sediment and nutrient loads at the outlet between September, 2010 and August, 2013.

Flood event	Water yield		Sediment		P		NO_3^-	
	(dam^3)	(%)	(t)	(%)	(kg)	(%)	(t)	(%)
Year: 2010/2011								
1	44.7	0.2	25.5	1.2	76.4	1.9	0.3	0.1
2	969.2	3.4	205.2	10.0	615.5	15.5	10.2	5.0
3	622.7	2.2	233.8	11.4	696.3	17.5	9.9	4.9
4	497.3	1.7	16.2	0.8	45.9	1.2	2.8	0.1
5	265.1	0.9	7.2	0.4	20.1	0.5	1.1	0.6
6	347.4	1.2	13.4	0.7	38.4	1.0	0.3	0.2
7	1473.1	5.1	317.5	15.4	812.1	20.4	7.4	3.6
8	975.2	3.4	255.9	12.4	758.3	19.1	0.6	0.3
9	170.9	0.6	72.2	3.5	216.4	5.4	7.5	0.4
Total (flood events)	5365.6	18.7	1146.9	55.8	3279.4	82.4	30.9	15.2
Total (year)	28737.9	–	2056.0	–	3978.0	–	204.8	–
Year: 2011/2012								
10	68.6	5.4	1.4	2.5	4.2	2.5	0.1	0.2
11	159.8	12.6	1.8	3.2	4.6	2.7	3.2	16.7
Total (flood events)	228.4	18.0	3.2	5.7	8.8	5.2	3.3	16.9
Total (year)	1269.8	–	56.3	–	168.0	–	19.7	–
Year: 2012/2013								
12	10.0	0.1	5.7	0.3	17	0.4	0.3	0.5
13	278.1	2.7	33.8	2.0	101.5	2.7	0.0	0.1
14	433.2	4.3	458.7	27.6	1356.3	35.8	0.7	1.0
15	145.1	1.4	27.5	1.7	82.5	2.2	0.5	0.7
16	262.0	2.6	35.2	2.1	105.7	2.8	1.5	2.2
17	108.9	1.1	41.1	2.5	123.4	3.3	3.0	4.4
18	2823.7	27.9	543.4	32.7	860.3	22.7	2.6	3.9
19	353.8	3.5	31	1.9	93.1	2.5	0.	0.8
20	429.4	4.2	61.8	3.7	185.4	4.9	2.0	2.9
21	1331.7	13.1	39.3	2.4	117.8	3.1	1.5	2.2
Total (flood events)	6175.9	60.9	1277.5	76.8	3043.0	80.4	12.7	18.7
Total (year)	10138.8	–	1662.4	–	3783.6	–	67.8	–

Table IV. Pearson correlation matrix between the variables associated to flood events[a].

	FD	W	TR	RD	R1	R5	R10	P_{aver}	P_{max}	T_{peak}
FD	1.00									
W	**0.83**	1.00								
TR	**0.48**	0.37	1.00							
RD	0.16	0.19	-0.11	1.00						
R1	-0.17	-0.13	**0.46**	-0.13	1.00					
R5	-0.26	-0.13	0.08	-0.08	**0.71**	1.00				
R10	-0.28	-0.17	-0.16	-0.11	**0.49**	**0.74**	1.00			
P_{aver}	0.33	**0.55**	0.10	0.32	0.00	0.19	0.03	1.00		
P_{max}	**0.43**	0.28	**0.40**	0.18	0.28	0.24	0.14	**0.54**	1.00	
T_{peak}	**0.60**	0.34	0.26	0.35	0.00	-0.23	-0.21	0.19	**0.53**	1.00

[a] FD, flood duration; W, water yield; RA, rainfall amount between the rising and recession limbs of a flood event; RD, rainfall duration in a flood event; R1, R5, and R10, cumulative precipitation in the 24h, five and ten days before the first discharge peak, respectively; P_{max}, discharge peak; T_{peak} and R_{peak} correspond to the duration and amount of rain accumulated since the beginning of the rain event until the discharge peak of a flood event, respectively.

.

Table V. Conceptual model of the source and transport of sediments and nutrients in the river Enxoé catchment area.

	Autumn			Winter			Spring			Summer		
	Source	**Transfer**	**Hysteresis pattern**	**Source**	**Transfer**	**Hysteresis pattern**	**Source**	**Transfer**	**Hysteresis pattern**	**Source**	**Transfer**	**Hysteresis pattern**
Particulate elements												
– **SSC, TP, and PP**	River banks	Runoff	Flushing Clockwise	Agricultural fields	Runoff	Flushing Mixed	River banks Agricultural fields	Runoff	Flushing Mixed	No flow	–	–
Soluble elements												
– **SRP**	River banks Agricultural fields	Runoff Lateral flow	Dilution Mixed	River banks	Runoff	Flushing Clockwise	River banks	Runoff	Flushing Clockwise	No flow	–	–
– **NO_3^-**	Agricultural fields	Lateral flow	Flushing Anticlockwise	Agricultural fields	Lateral flow	Dilution Mixed	Agricultural fields	Lateral flow	Dilution Anticlockwise	No flow	–	–

SSC, suspended sediment concentration, TP, total phosphorous, PP, particulate phosphorous, SRP, soluble reactive phosphorous, NO_3^-, nitrate.

Table VI. Annual water, sediment, and nutrient yields in the Enxoé catchment between September, 2010 and August, 2013.

	Outputs					
	2010/2011		**2011/2012**		**2012/2013**	
Water yield (mm)						
– **river discharge**	473	(62.6%)	21	(6.5%)	167	(26.5%)
Sediments (kg ha^{-1})	338.2		9.3		273.4	
P (kg ha^{-1})	0.65	(4.4%)	0.03	(0.2%)	0.62	(4.2%)
N (kg ha^{-1})	7.61	(14.9%)	0.73	(1.4%)	2.52	(4.9%)

List of Figures

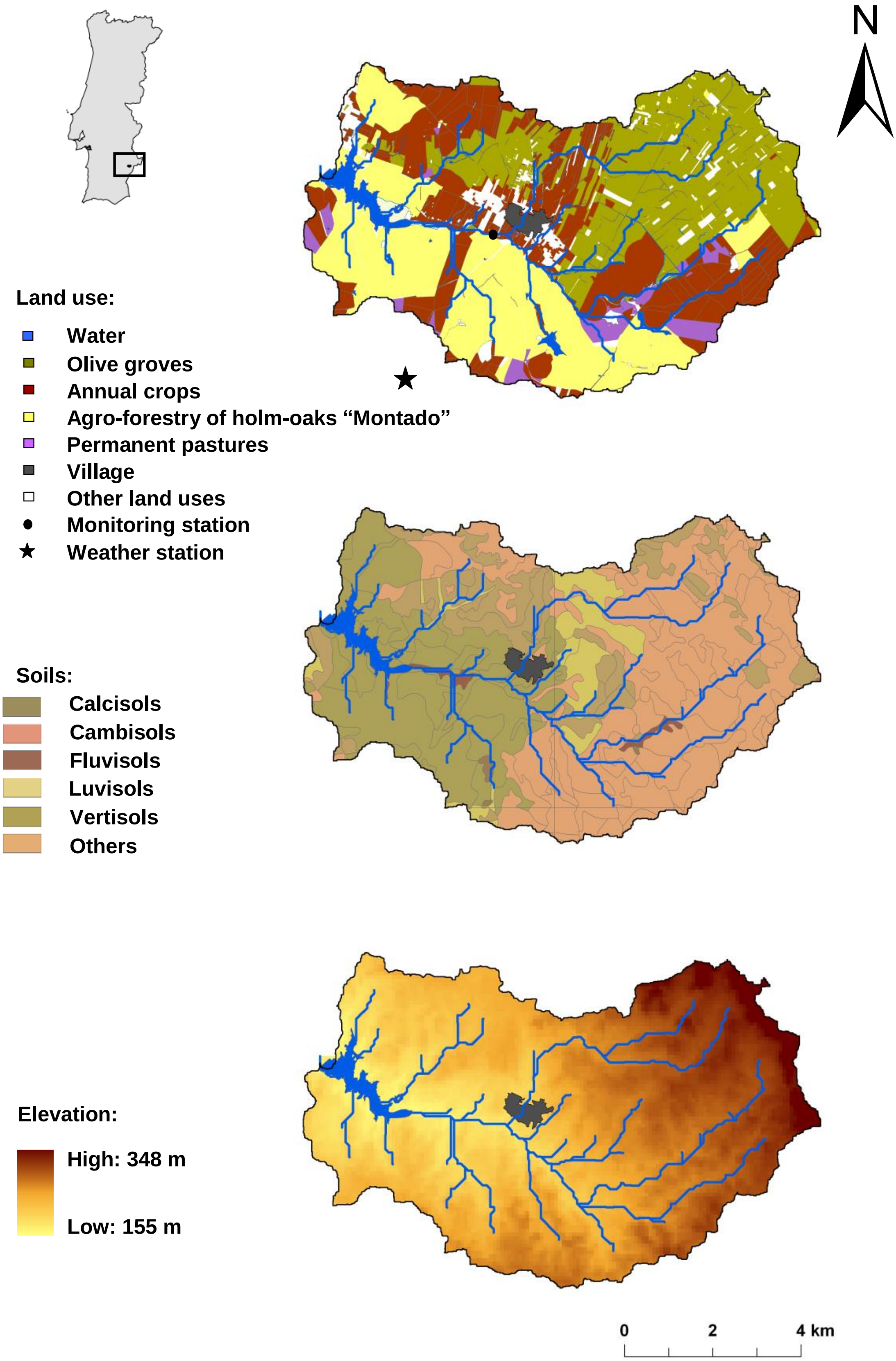

Figure 1. Location and land use (top), major soil units (middle), and digital elevation model (bottom) in Enxoé catchment area.

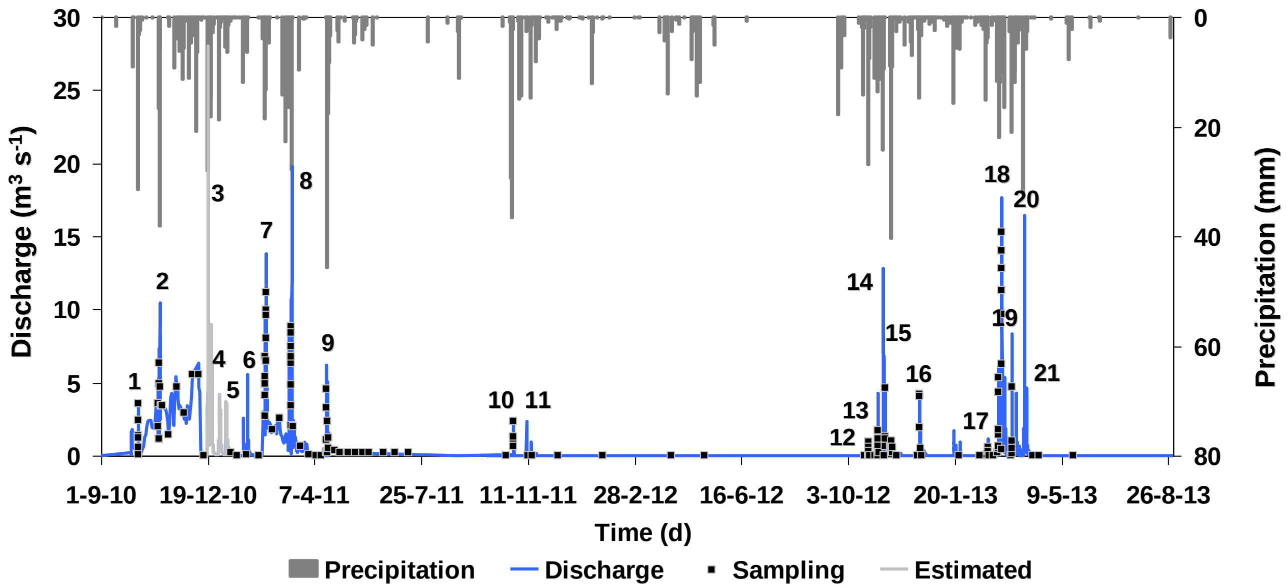

Figure 2. Precipitation (mm) and discharge (m^3 s^{-1}) at the river Enxoé outlet between September, 2010 and August, 2013. Line in light grey represents a period of 22 days when the equipment malfunctioned.

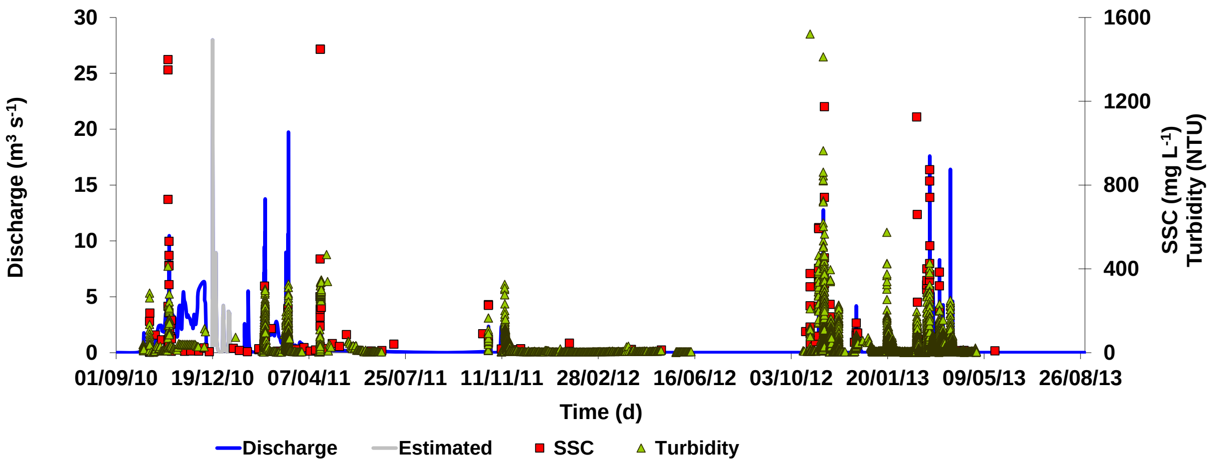

Figure 3. Discharge, suspended solid concentration (SSC), and turbidity monitored between September, 2010 and August, 2013. Line in light grey represents a period of 22 days when the equipment malfunctioned.

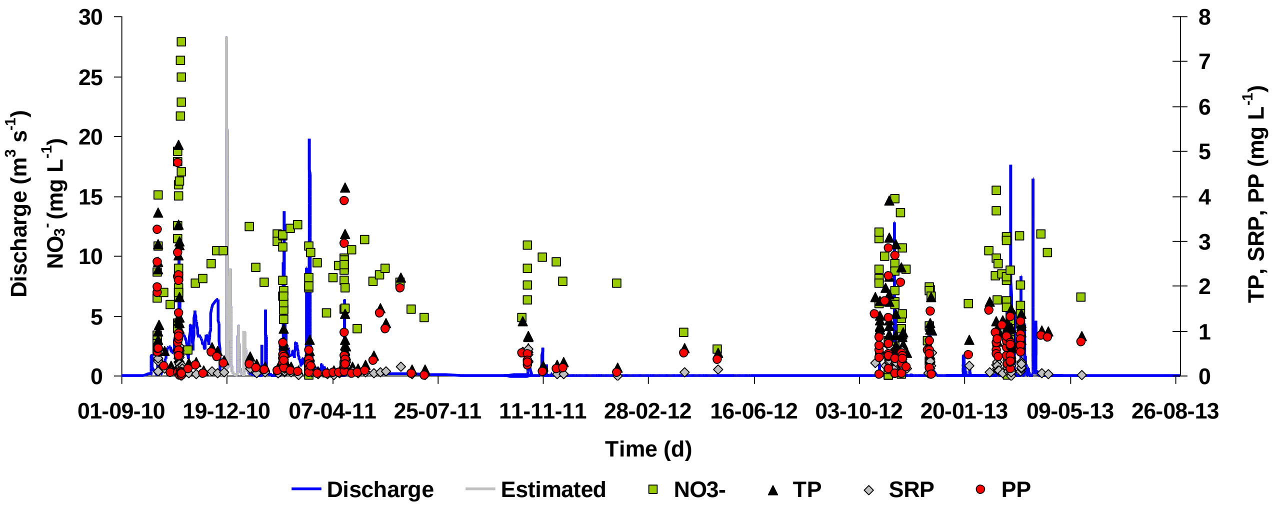

Figure 4. Discharge, nitrate (NO_3^-), total (TP), particulate (PP) and soluble reactive (SRP) phosphorous concentrations observed between September, 2010 and August, 2013. Line in light grey represent a period of 22 days when the equipment malfunctioned.

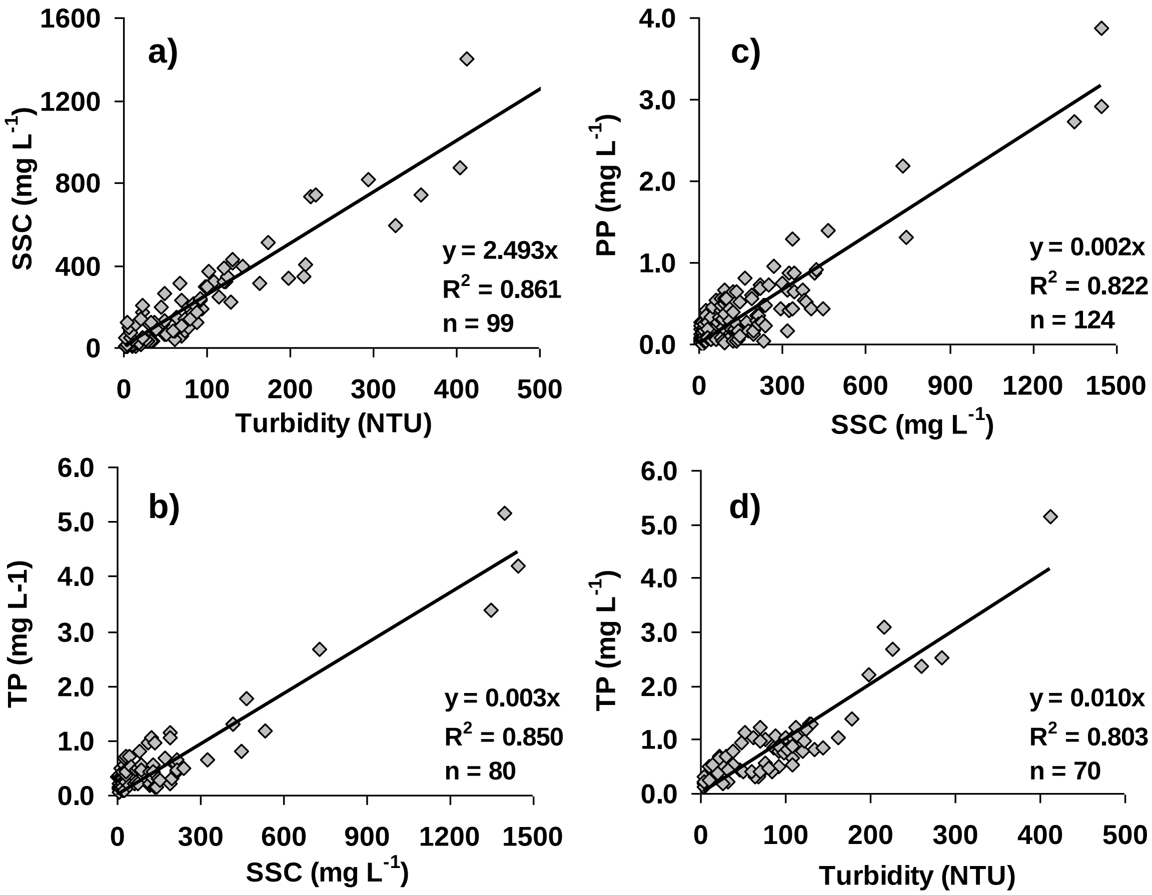

Figure 5. Regression analysis between (a) suspended solid concentration (SSC) and turbidity; (b) total phosphorous (TP) and SSC; (c) particulate phosphorous (PP) and SSC; and (d) TP and turbidity.

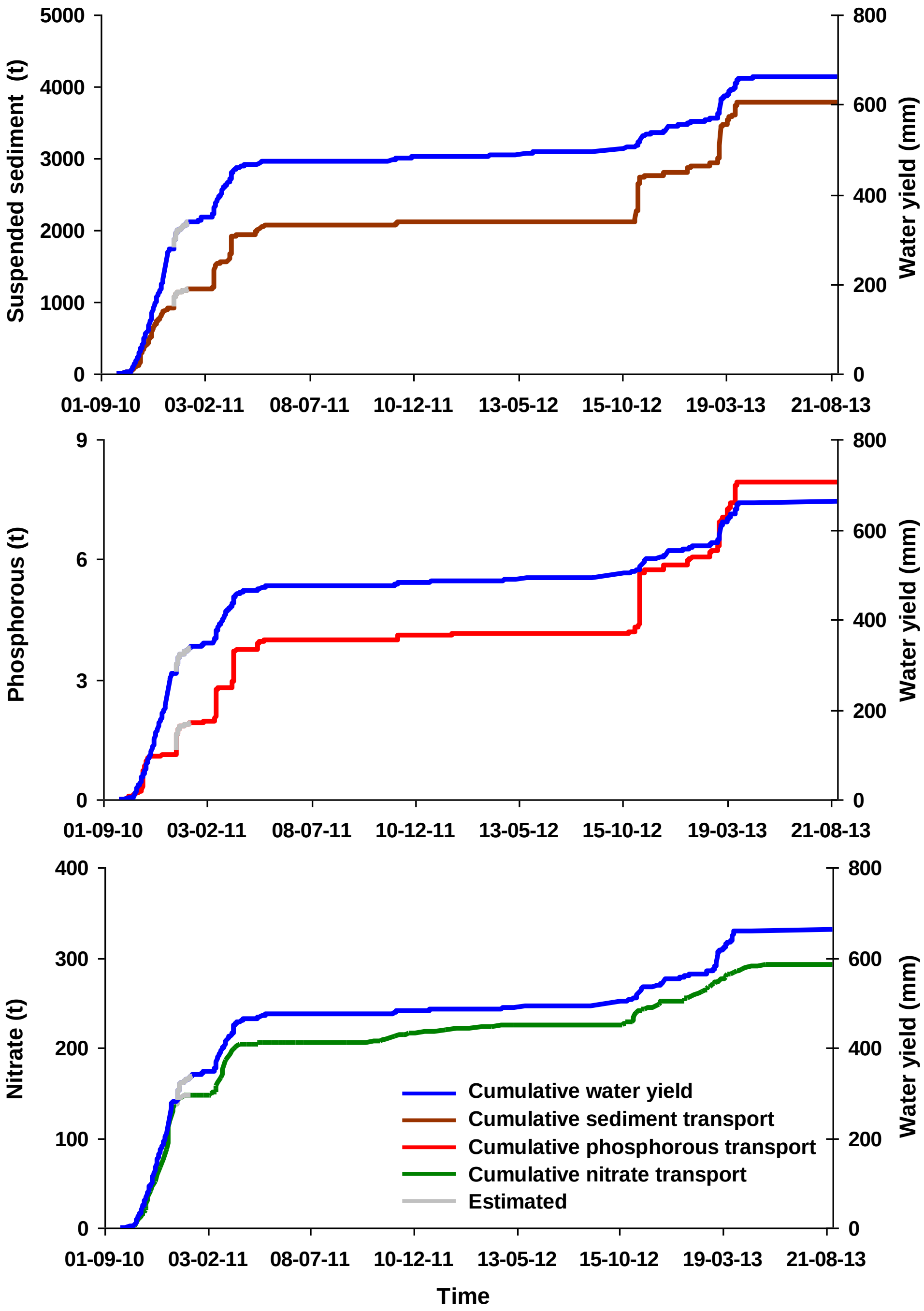

Figure 6. Cumulative water yield (mm), suspended sediments (t), phosphorous (t), and nitrate transport in the Enxoé catchment between September, 2010 and August, 2013.

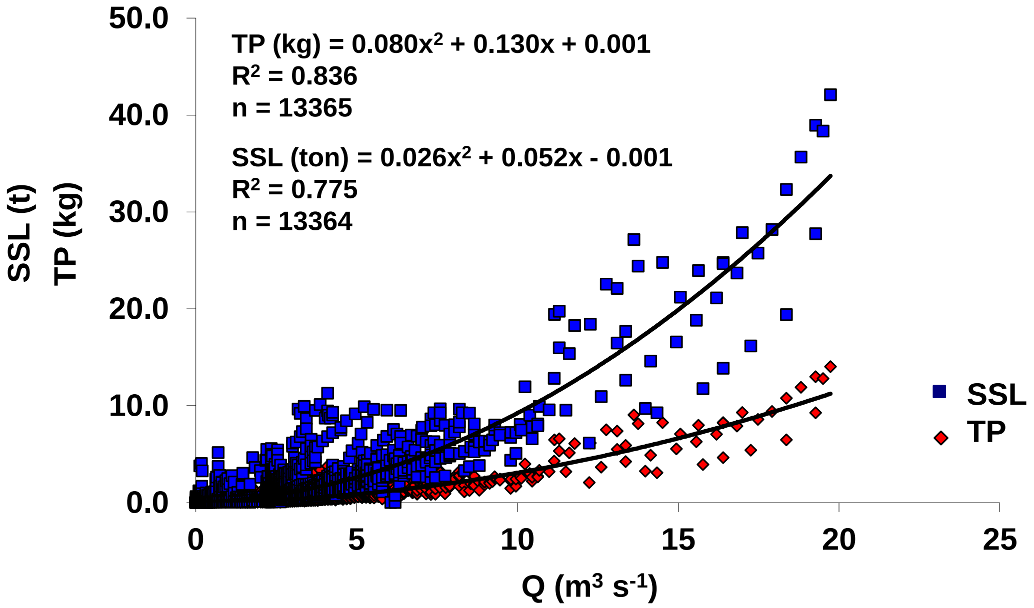

Figure 7. Relations between suspended sediment loads (SSL), or total phosphorous (TP) loads, and discharge (Q) in the Enxoé catchment.

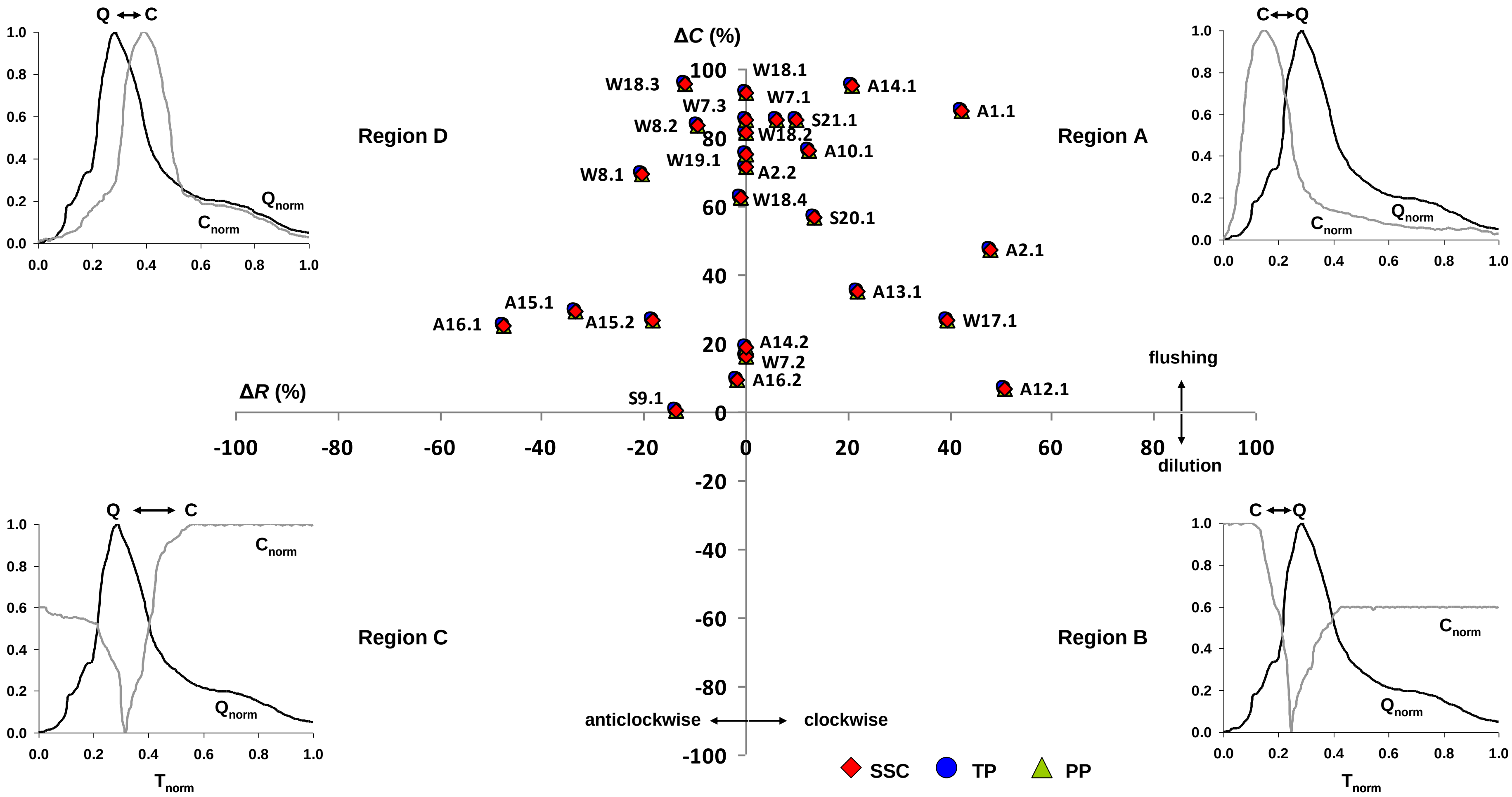

Figure 8. Unity plane Δ*C* vs. Δ*R* for the *C*-*Q* hysteresis loops of suspended solid concentration (SSC), total phosphorous (TP), and particulate phosphorous (PP). The marks *i*,*j* correspond to the i^{th} flood event monitored (1-21) and the j^{th} discharge peak (1-4) monitored during autumn (A), winter (W), and spring (S). Typical *C*-*Q* relations are presented for each region of the unity plane Δ*C* vs. Δ*R*.

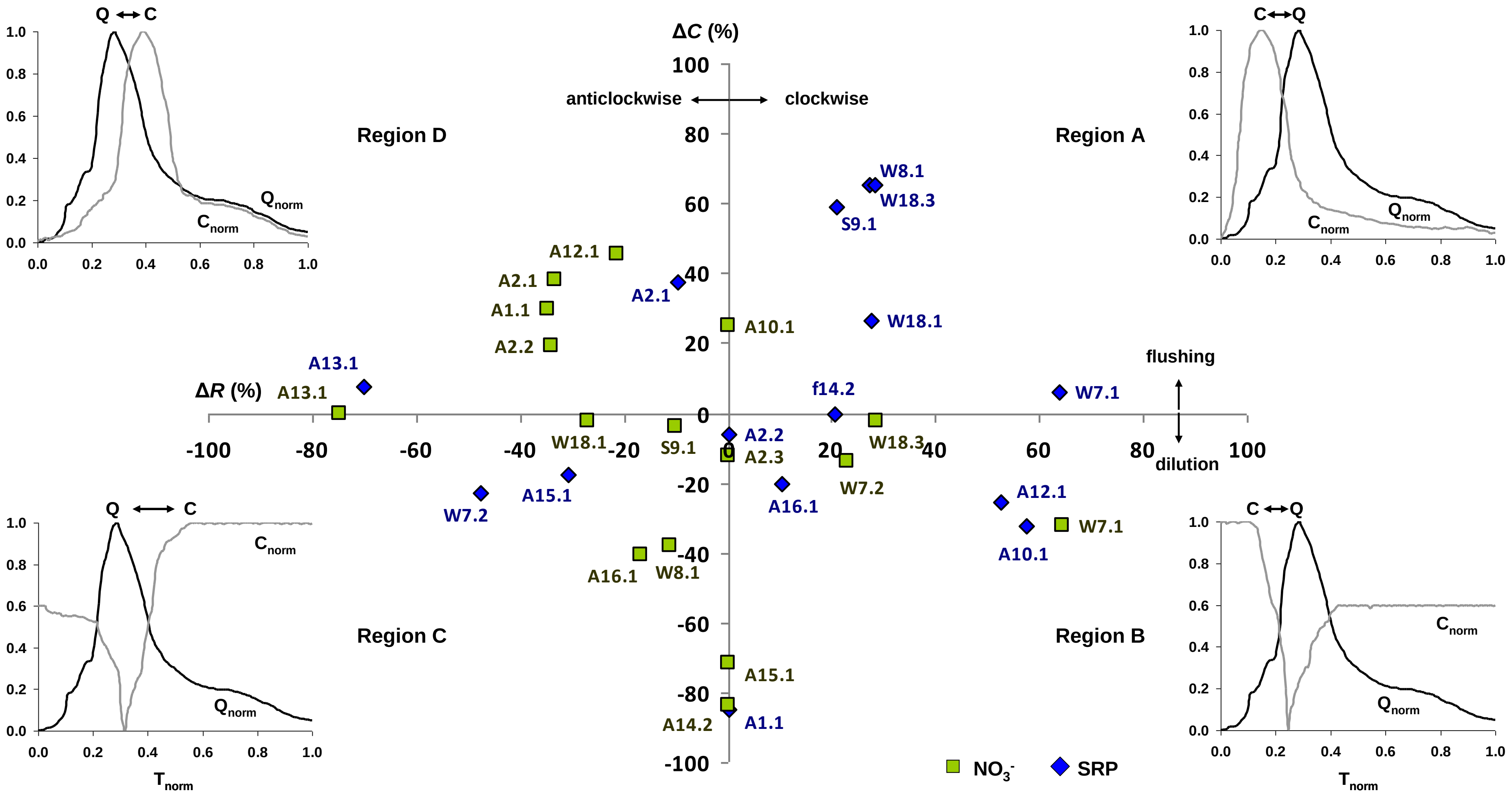

Figure 9. Unity plane Δ*C* vs. Δ*R* for the *C*-*Q* hysteresis loops of soluble reactive phosphorous (SRP), and nitrate (NO_3^-). The marks *i*,*j* correspond to the i^{th} flood event monitored (1-21) and the j^{th} discharge peak (1-4) monitored during autumn (A), winter (W), and spring (S). Typical *C*-*Q* relations are presented for each region of the unity plane Δ*C* vs. Δ*R*.